Journal of Macromolecular Science, Part A
Publication details, including instructions for authors and subscription information:
http://www.informaworld.com/smpp/title~content=t713597274

Enhanced Adsorption of Ammonium Using Hydrogel Composites Based on Chitosan and Halloysite

Yian Zheng[a]; Aiqin Wang[a]
[a] Chinese Academy of Sciences, Center for Eco-material and Green Chemistry, Lanzhou Institute of Chemical Physics, Lanzhou, China

To cite this Article Zheng, Yian and Wang, Aiqin(2010) 'Enhanced Adsorption of Ammonium Using Hydrogel Composites Based on Chitosan and Halloysite', Journal of Macromolecular Science, Part A, 47: 1, 33 — 38

To link to this Article: DOI: 10.1080/10601320903394421

URL: http://dx.doi.org/10.1080/10601320903394421

Journal of Macromolecular Science®, Part A: Pure and Applied Chemistry (2010) **47**, 33–38
Copyright © Taylor & Francis Group, LLC
ISSN: 1060-1325 print / 1520-5738 online
DOI: 10.1080/10601320903394421

Enhanced Adsorption of Ammonium Using Hydrogel Composites Based on Chitosan and Halloysite

YIAN ZHENG and AIQIN WANG*

Center for Eco-material and Green Chemistry, Lanzhou Institute of Chemical Physics, Chinese Academy of Sciences, Lanzhou, 730000, China

Received May 2009, Accepted June 2009

In this work, chitosan was used as the backbone to graft poly(acrylic acid) to form granular hydrogel composite with halloysite (HT) particles being embedded within the polymeric networks. This hydrogel composite was characterized by means of Fourier-transform infrared spectroscopy (FTIR), X-ray diffraction (XRD), scanning electron microscopy (SEM), and thermogravimetric analysis (TGA). Then, this hydrogel composite was selected as the adsorbent to remove ammonium from synthetic wastewater. The results indicate that by introducing HT particles into the polymeric networks, the resulting composite shows comparable adsorption capacity to that of pure polymer hydrogel for NH_4^+ removal. The adsorption equilibrium can be achieved within 5 min with the equilibrium adsorption capacity of 27.7 mg N/g and monolayer adsorption capacity of 40.9 mg N/g (30 wt% HT). The adsorption process is pH-independent within 4.0–7.0, and the adsorption capacity of as-prepared adsorbent is not affected over the cycles of adsorption studied (5 cycles).

Keywords: Adsorption, ammonium, chitosan, halloysite, hydrogel composite

1 Introduction

Chitosan (CTS) is a *N*-deacetylated derivative of chitin (poly-β-(1→4) linked *N*-acetylglucosamine) which is considered as the second most abundant compound in nature after cellulose. CTS has good antimicrobial, antibacterial, antifungal and biodegradable features, and also, due to the presence of chemical reactive groups (primary, secondary hydroxyl groups and highly reactive amino groups), CTS can be easily modified, in particular crosslinking and grafting reactions, by which some novel functions can be introduced into this biopolymer (1–3). CTS and its derivatives have been studied widely and can be considered as the candidates in many fields, such as controlled drug release (4), food preservation (5), bio- or electrochemical sensors (6, 7), alkaline fuel cells (8), durable press finishing (9), superabsorbents (10), tissue engineering (11), adsorbents (12, 13) and flocculants (14). In addition, CTS has increased interest as the backbone to graft vinyl monomers or other functional polymer to widen its further applications. For example, CTS can be grafted as copolymerized with acrylonitrile and methylmethacrylate to form thin membranous films, which may be usable as biodegradable packaging materials (15). Adali et al. used CTS as the backbone to graft poly(ethylene glycol dimethacrylate), and the product can potentially be used for external intervention devices on bone and other tissue (16).

Polymeric hydrogels are defined as water-swollen, three-dimensional structured polymers. CTS-based hydrogels are one branch of polymeric hydrogels, which can be easily prepared via *in situ* copolymerization in aqueous solution using CTS as the backbone to graft synthesized monomers, such as acrylic acid (10). The resulting product is granular, which is very different from common polymeric hydrogels with the formation of gel-form products requiring much energy for drying and crushing. Considering the limitations of pure polymeric hydrogels, such as poor gel strength and stability, some inorganic clays such as attapulgite (17), montmorillonite (18), vermiculite (19) and sepiolite (20) have been incorporated into the hydrogel matrix. Clays are natural, abundant and inexpensive materials that have high mechanical strength and chemical resistance. Halloysite (HT) is a two-layered aluminosilicate, chemically similar to kaolin, which has a predominantly hollow tubular structure in the submicrometer range. The neighboring alumina and silica layers and their waters of hydration create a packing disorder causing them to curve (21). HT is an economically

---

*Address correspondence to: A. Wang, Center for Eco-material and Green Chemistry, Lanzhou Institute of Chemical Physics, Chinese Academy of Sciences, Lanzhou, 730000, China. Tel.: 86/931/4968118; Fax: 86/931/8277088; E-mail: aqwang@lzb.ac.cn

viable raw material and due to its unique nanotubular characteristic, HT has been used widely in many fields including biomimetic nanoreactor (21), controlled drug and protective agent release (22–24), modification of polypropylene (25) and water treatment (26). However, to the best of our knowledge, little information is reported using HT as an inorganic component to prepare polymeric hydrogel composite.

Due to peculiar characteristics, polymeric hydrogels have been used as adsorbents to remove hazardous metal ions or ionic dyes (27). These hydrogels are hydrophilic but not dissolved in water, making them easily separated from the aqueous solution. Furthermore, the presence of a large number of multifunctional ionic groups within these hydrogels affords them surprising affinity to pollutants in the surrounding water environment. However, no information has been reported using this type of hydrogel adsorbent to remove ammonium (NH_4^+) which is the inorganic ion form of nitrogen pollution and is one of the limiting factors causing eutrophication (28). Based on the above background, in this study, a polymeric hydrogel composite based on CTS, nanotubular HT and acrylic acid was developed and its structure was well investigated by means of FTIR, XRD, SEM and TGA technologies. Then, the adsorption characteristics of this type of adsorbent for NH_4^+ from the aqueous solution were evaluated.

2 Experimental

2.1 Materials

Acrylic acid (AA, chemically pure, Shanghai Shanpu Chemical Factory, Shanghai, China) was distilled under reduced pressure before use. Ammonium persulfate (APS, analytical grade, Sinopharm Chemical Reagent Co., Ltd., Shanghai, China), *N*, *N*′-methylene-bisacrylamide (MBA, chemically pure, Shanghai Yuanfan additives plant, Shanghai, China), chitosan (CTS, with an degree of deacetylation of 0.85 and average molecular weight of 3×10^5, Zhejiang Yuhuan Ocean Biology Co., Zhejiang, China) and powdered activated carbon were used as received. Halloysite (HT, Zhengzhou Golden Sunshine Ceramics Co., Ltd., Henan, China) was milled through a 200-mesh screen prior to use, with a chemical composition of analytical Al_2O_3 51.12 wt%, SiO_2 47.35 wt%, Na_2O 0.786 wt%, K_2O 0.362, CaO 0.23 wt% and Fe_2O_3 0.15 wt%.

A 1000 mg/L stock standard solution of NH_4^+ was prepared by dissolving an appropriate amount of ammonium chloride (dried to a constant mass at 100–105°C) in 1000 mL of distilled water. A series of working standard solutions were prepared by appropriate dilution of the stock solution. The initial pH value was adjusted by the addition of diluted NaOH or HCl solution to a desired value (Mettler Toledo FE20 pH-meter). Other reagents used were all analytical grade and all solutions were prepared with distilled water.

2.2 Hydrogel Preparation

An appropriate amount of CTS (0.5 g) was dissolved in a mixing solution which consisted of AA (3.6 g), MBA (0.15 g), and distilled water (45 mL) in a 250 mL flask equipped with a stirrer, condenser, thermometer and a nitrogen line. This solution was heated to 60°C gradually and kept for 30 min, and then a calculated amount of HT was put into the reactor. After removal of oxygen (20 min), initiator solution containing 0.1 g APS was added to initiate CTS to generate radicals. During this process, the mixture was heated to 70°C and kept for 3 h to complete the polymerization reaction. When the reaction was finished, the resulting granular product was neutralized with sodium hydroxide solution to neutral pH, dehydrated with industrial alcohol and dried at 70°C to a constant weight. The adsorbent used for the test had a particle size of 40–80 mesh. The digital photos of hydrogels with and without HT were shown in Figure 1.

2.3 Characterization

FTIR spectra were recorded on a Thermo Nicolet NEXUS TM spectrophotometer using KBr pellets in the range of $4000\ cm^{-1}$–$400\ cm^{-1}$. XRD patterns were obtained from an X′Pert PRO diffractometer (CuKα radiation, 40 kV, 30 mA). SEM studies were carried out in a JSM-5600LV SEM instrument (JEOL, Ltd.) after coating the sample with gold film using an acceleration voltage of 20 kV. Thermal stability studies were performed on a Perkin-Elmer TGA-7 thermogravimetric analyzer, in the temperature range 26-700°C at a heating rate of 10°C/min using dry nitrogen purge at a flow rate of 50 mL/min.

2.4 Adsorption Experiment

Adsorption measurements were determined by contacting a 50 mg sample with 25 mL NH_4^+ solutions. The

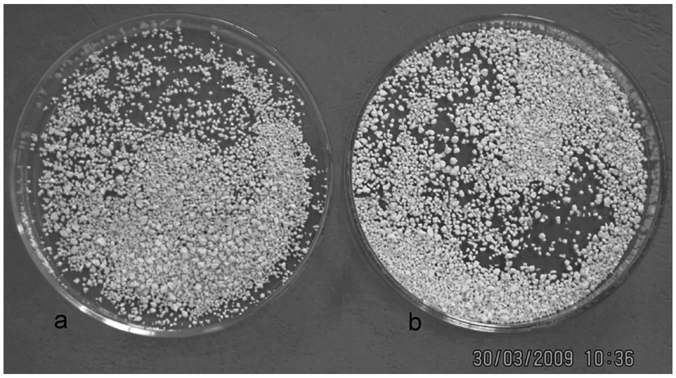

Fig. 1. Digital photos of CTS-*g*-PAA (a) and CTS-*g*-PAA/30 wt% HT (b).

mixtures were shaken in a thermostatic shaker (THZ-98A) at 30°C/120 rpm for a given time, and then the suspensions were centrifuged at 4500 rpm for 10 min. The experiments were carried out by varying contact time, NH_4^+ concentration and initial pH values. The NH_4^+ concentration in the solution was measured according to Nessler's reagent colorimetric method. The adsorption capacity for NH_4^+ was calculated from the following equation (Equation 1):

$$qe = \frac{(C_0 - C_e)V}{m} \tag{1}$$

Where q_e is the adsorption capacity of NH_4^+ onto adsorbent (mg N/g), C_0 is the initial NH_4^+ concentration (mg N/L), C_e is the equilibrium NH_4^+ concentration (mg N/L), m is the mass of adsorbent used (mg), and V is the volume of NH_4^+ solution used (mL).

The reusable ability was determined according to the following procedures: (i) 50 mg of dried adsorbent was immersed in 25 mL NH_4^+ solution (100 mg N/L) and shaken in a thermostatic shaker at 30°C/120 rpm for 30 min; then, the suspension was centrifuged at 4500 rpm for 10 min. The analytical result was recorded as the first adsorption capacity; (ii) NH_4^+-loaded adsorbent was separated from the NH_4^+ solution and stirred in 25 mL 0.1 mol/L NaOH solution for 10 min. After centrifugation, the adsorbent was eluted with 20 mL distilled water several times. The obtained swollen adsorbent was then used as the adsorbent to contact again with 25 mL NH_4^+ solution and shaken in a thermostatic shaker at 30°C/120 rpm for 30 min to obtain the second adsorption capacity; (iii) A similar procedure was repeated and after several times, the adsorption capacity was then achieved.

3 Results and Discussion

3.1 FTIR Analysis

As shown in Figure 2, in the region of 3300 cm^{-1} to 3500 cm^{-1}, CTS exhibits a band corresponding to the stretching of –OH groups. This band is broad because of the hydrogen bonds. The –OH band overlaps the stretching band of N–H. The characteristic absorption bands at 1632 and 1323 cm^{-1} are assigned to overlapped amide (I and II) and amide III. In the region from 1000 cm^{-1} to 1200 cm^{-1}, CTS presents a broad band centered at 1090 cm^{-1}, corresponding to the stretching of C–O bond of C-3 from CTS (secondary OH). The band at 1033 cm^{-1} is produced by the C–O stretching of C-6 of CTS (primary OH). The band at 1090 cm^{-1} corresponds to the symmetric stretching of C–O–C, while the asymmetric stretching of C–O–C appears at 1155 cm^{-1}. After reaction, the absorption intensities at 1632 and 1090 cm^{-1} decrease and even \ disappear, suggesting that both $-NH_2$ and –OH groups of CTS participate in the reaction by which PAA is grafted onto the backbone of CTS. The new absorption bands at 1454 cm^{-1} (C–H) and 1411 cm^{-1} (symmetric $-COO^-$ stretching) are powerful evidence of PAA existence. In addition, the spectrum of pure HT exhibits two Al_2OH stretching bands at 3695 and 3619 cm^{-1}, each -OH being linked to two Al atoms (29), two types of water resulting in water –OH stretching bands at 3600 and 3553 cm^{-1} (30), a single water deformation vibration appeared at 1635 cm^{-1}, a single Al_2OH bending band at 908 cm^{-1}, and band at 1027 cm^{-1} attributed to Si–O–Si stretching vibrations. Compared with pure HT, the FTIR spectrum of resulting composite contains all of the above-mentioned adsorption bands except for disappeared or overlapped –OH bands. Consequently, it can be concluded that during the reaction, PAA is grafted onto the backbone of CTS and HT is successfully incorporated into the polymeric networks.

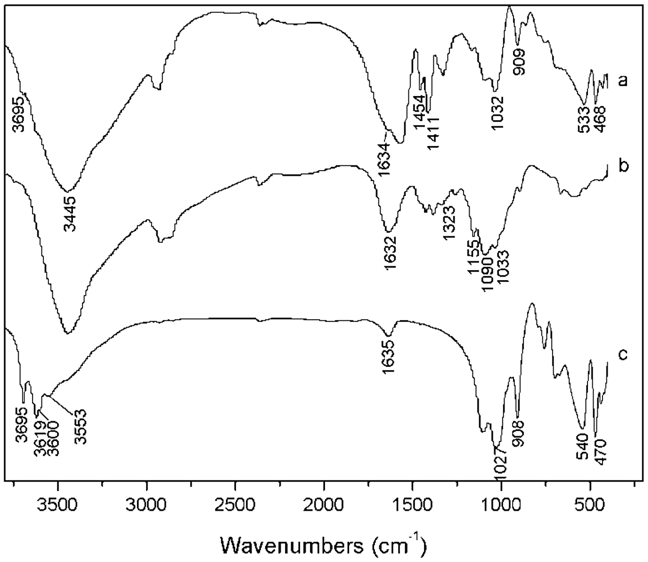

Fig. 2. FTIR spectra of (a) CTS-*g*-PAA/30 wt% HT, (b) CTS, and (c) halloysite.

3.2 XRD Analysis

XRD technologies are used to identify the presence of HT in the composite and the basal (d_{001}) reflections are indication of fully hydrated (10 Å), partially hydrated (7–10 Å), and dehydrated (7 Å) HT. As shown in Figure 3, the basal spacing reflections indicate a sharp peak at $2\theta = 11.80°$, which translates to a 001 basal spacing of 7.50 Å. However, no peak is observed at $2\theta = 8.76°$ indicating the absence of the 10 Å-form. So, HT used in this study was in the form of partially hydrated state. After polymerization, this typical diffraction peak can still be detected at the same 2θ but for a significant decrease in the peak intensity, indicative of lower content of HT in the composite which can be evidenced by comparing the XRD patterns of the physical mixture of HT and CTS-*g*-PAA (Figure 3b) and the resulting composite CTS-*g*-PAA/HT (Figure 3c). It is clear

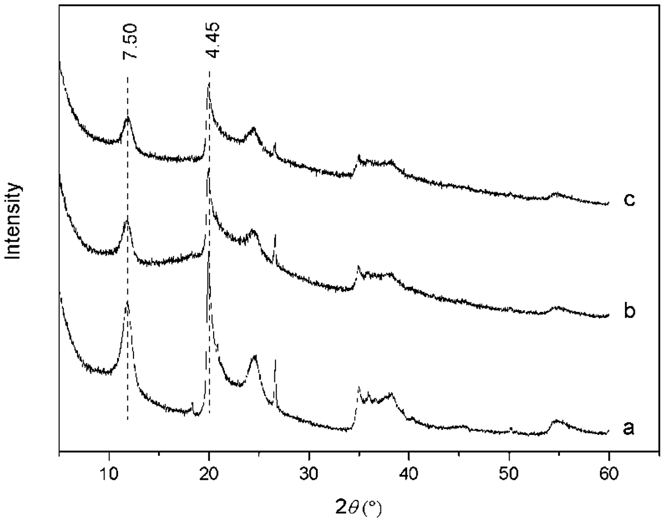

Fig. 3. XRD powder patterns of (a) halloysite, (b) halloysite/CTS-*g*-PAA (w/w, 3:7), and (c) CTS-*g*-PAA/30 wt% HT.

that no visible changes were observed. Therefore, it can be established that during the copolymerization, HT particles are dispersed within the polymeric networks without any interference. In addition, the presence of the very intense reflection at ∼4.45 Å is the diagnostic feature of common tubular morphology within HT and its composite (26, 31).

3.3 SEM Analysis

Figure 4 shows the micrographs of CTS-*g*-PAA hydrogels with and without HT. It is clearly observed that CTS-*g*-PAA shows a smooth and tight surface with some micro-pores decorated on the surface. However, the samples incorporated with HT exhibit a different coarse surface on which many micro-pores are observed. An undulant and coarse surface can benefit for water permeation, making the adsorbate molecules easily diffuse into the composite, and accordingly, the final adsorption capacity would be improved.

3.4 Thermal Stability

The thermal stabilities of CTS-*g*-PAA and CTS-*g*-PAA/HT are tested by TGA, and their TGA and DTG curves in nitrogen atmosphere are shown in Figure 5. When 10% and 20% weight losses are achieved, the corresponding temperature is found to be 141 and 311°C for CTS-*g*-PAA, while for CTS-*g*-PAA/HT, they are observed to be 178 and 313°C, respectively. In addition, the major weight losses of CTS-*g*-PAA and CTS-*g*-PAA/HT are located at the temperature of 441 and 446°C. The results indicate that the addition of HT into the pure CTS-*g*-PAA polymeric networks can improve the thermal stability. This is due to that the incorporation of inorganic component can produce the barrier effect, making some small molecules generated during the thermal decomposition cannot permeate, and thus have to bypass the obstacles due to HT particles.

3.5 Adsorption

During the experiment, it is found that HT has no adsorption for NH_4^+. Then, the adsorption capacity is calculated based on *g*-polymer to make a convenient and significant comparison with pure polymer hydrogel CTS-*g*-PAA. The results suggest that the respective adsorption capacity for NH_4^+ is 25.9, 27.7, 39.5 and 41.0 mg N per gram

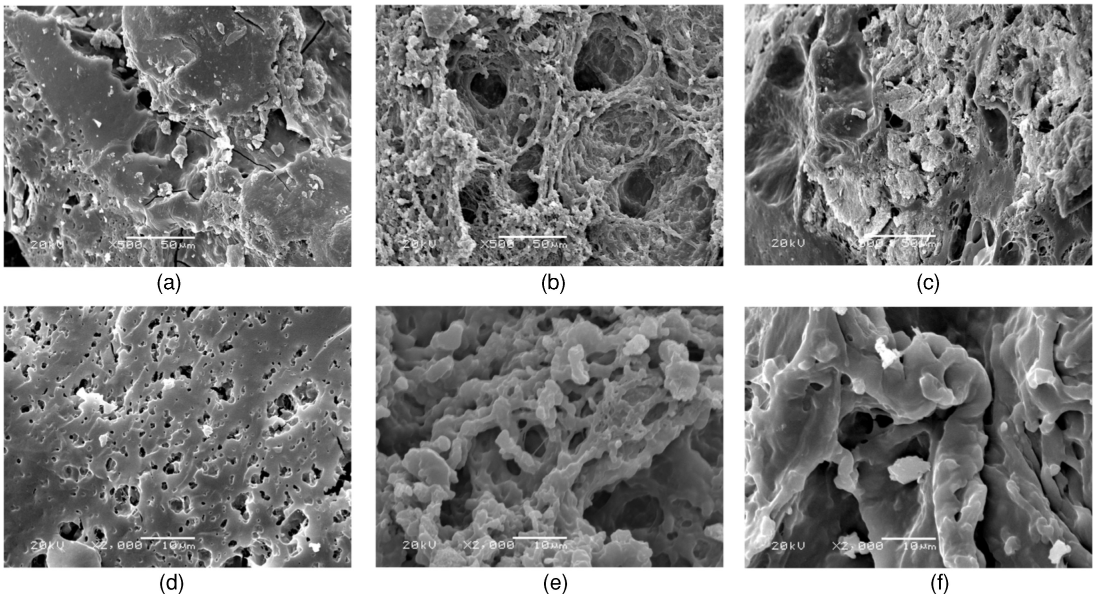

(a) (b) (c)
(d) (e) (f)

Fig. 4. Scanning electron micrographs for dried hydrogel composite: (a) CTS-*g*-PAA (500×), (b) CTS-*g*-PAA/10 wt% HT (500×), (c) CTS-*g*-PAA/30 wt% HT (500×), (d) CTS-*g*-PAA (2000×), (e) CTS-*g*-PAA/10 wt% HT (2000×), and (f) CTS-*g*-PAA/30 wt% HT (2000×).

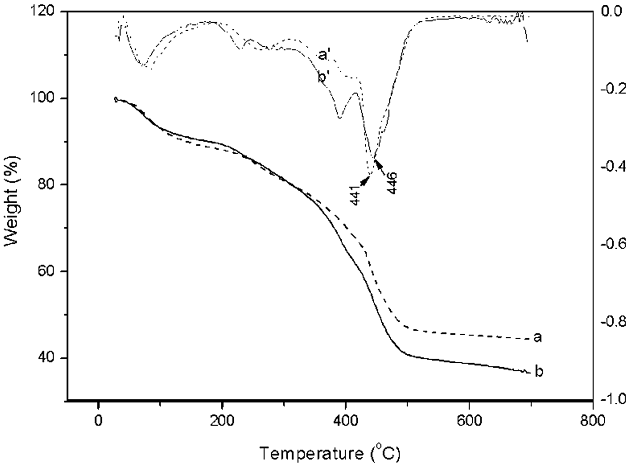

Fig. 5. TGA and DTG curves of hydrogel adsorbent. a (a′), CTS-*g*-PAA; b (b′), CTS-*g*-PAA/30 wt% HT.

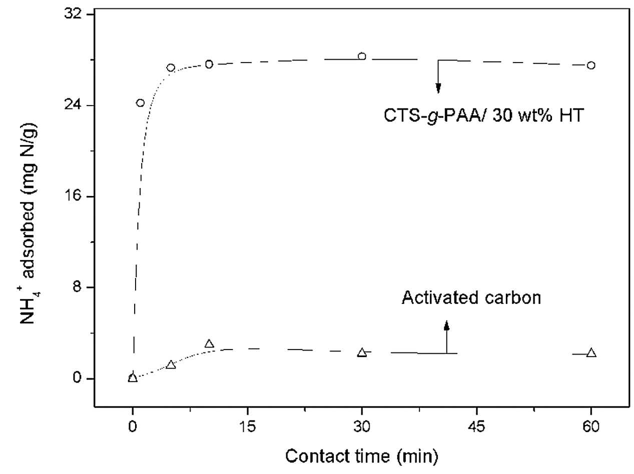

Fig. 6. Effect of contact time on adsorption capacity (Adsorption conditions: 30°C, 200 mg N/L, pH 6-7, 120 rpm).

of *g*-polymer using CTS-*g*-PAA, CTS-*g*-PAA/10 wt% HT, CTS-*g*-PAA/30 wt% HT and CTS-*g*-PAA/50 wt% HT as the adsorbent. That is, by introducing HT into the polymeric networks, corresponding hydrogel composite shows a more improved adsorption capacity than that of pure polymer hydrogel CTS-*g*-PAA, especially when more inorganic HT particles are added. Considering the higher adsorption capacity and proper amount of HT, CTS-*g*-PAA/30 wt% HT was selected for further studies.

For an adsorbent, the rapid adsorption and high capacity are desirable properties. Preliminary experiments show that the adsorption capacity would not be affected within pH 4.0–7.0, and then in this section, the adsorption kinetics of as-prepared adsorbent for NH_4^+ adsorption were investigated and compared with activated carbon, as shown in Figure 6. The result indicated that 1–3 mg N/g of adsorption capacity was observed for activated carbon during the contact time investigated, while for hydrogel adsorbent, >85% NH_4^+ could be adsorbed within 1 min, and the equilibrium was achieved approximately within 5 min, meaning it is a quite fast adsorption process. This is because that as-prepared adsorbent consisted of flexible polymeric chains with super-hydrophilic characteristics. When it is immersed in an aqueous solution, water molecules penetrate quickly into the gel and dissociate –COOH groups to $-COO^-$ groups, resulting in a dimensional increase of polymeric networks. Then, the concentration gradient of NH_4^+ is formed at gel-water interface, and the diffusion of NH_4^+ into the gel is started. Due to the presence of ionic functional groups, NH_4^+ moved from the external solution into the gel can be adsorbed and trapped within the polymeric networks, causing the adsorption system to reach equilibrium within a few minutes. When the adsorption equilibrium was attainable, the adsorption capacity was found to be 27.7 mg N/g for CTS-*g*-PAA/30 wt% HT, that is, 39.5 mg N per gram of polymer.

The adsorption of NH_4^+ onto CTS-*g*-PAA/30 wt% HT determined as a function of equilibrium NH_4^+ concentration is plotted in Figure 7. It can be clearly seen that the NH_4^+ adsorption capacity increased with increasing the equilibrium NH_4^+ concentration. This is attributed to the fact that an increase in NH_4^+ concentration accelerates the diffusion of NH_4^+ molecules into the polymeric networks as a result of an increase in the driving force of concentration gradient. The adsorption isotherms reveal the specific relation between the concentration of adsorbate and the adsorption capacity of an adsorbent at a constant temperature. In this study, equilibrium adsorption isotherm data were analyzed according to Langmuir model (Equation 2) to find the monolayer adsorption capacity of

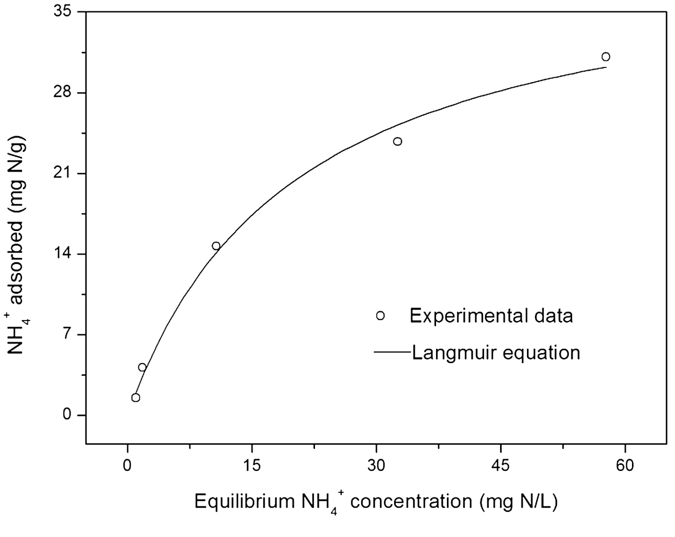

Fig. 7. The change of adsorption capacity as a function of equilibrium NH_4^+ concentration (Adsorption conditions: 30°C, 30 min, pH 6–7, 120 rpm).

hydrogel composite for NH_4^+:

$$q_e = \frac{q_m b C_e}{1 + bC_e} \quad (2)$$

Where q_e is the equilibrium adsorption capacity of NH_4^+ on adsorbent (mg N/g), C_e is the equilibrium NH_4^+ concentration (mg N/L), q_m is the monolayer adsorption capacity of the adsorbent (mg N/g) and b is the Langmuir adsorption constant (L/mg). By non-linear regression of the experimental data, the calculated monolayer adsorption capacity of NH_4^+ onto CTS-*g*-PAA/30 wt% HT is as high as 40.9 mg N/g with $b = 4.93 \times 10^{-2}$ L/mg and correlation coefficient $R^2 = 0.9937$, meaning that the Langmuir model fits the adsorption data well.

Reusing ability and stability of an adsorbent during the regeneration process are important parameters. NH_4^+-loaded sample was treated with 0.1 mol/L NaOH as described in the experimental part and used again in adsorption of NH_4^+ to observe these properties. Here, it should be mentioned that it is quite easy for the adsorbed NH_4^+ to be desorbed from the samples and the adsorbed NH_4^+ can be completely desorbed within 10 min using 0.1 mol/L NaOH as the eluent. After five cycles of adsorption, the sample shows almost the same NH_4^+ adsorption capacity under the current experimental conditions. That is to say, the sample has the excellent reusing ability and can maintain greater stability during the regeneration process.

4 Conclusions

In this study, a series of hydrogel composites consisted of CTS, nanotubular HT and AA were prepared. FTIR analysis suggests that during the copolymerization, PAA has grafted onto the backbone of CTS, and HT particles are successfully embedded within the polymeric networks. XRD analysis reveals that the HT used in this study is in the form of partially hydrated state, and no additional interaction is present among the reactants. SEM analysis shows that by introducing HT into the hydrogel, the sample surface becomes coarse and many micro-pores are visible, which can contribute to its adsorption for NH_4^+. TGA analysis implies that the addition of HT particles can improve the thermal stability of pure polymeric hydrogel. For this hydrogel composite, well-formed three-dimensional structured polymeric networks are responsible for its faster adsorption kinetics, and the presence of the hydrophilic anionic groups on the chains are considered the governed mechanism for the higher adsorption capacity for NH_4^+ removal. As-prepared adsorbent shows pH-independence within 4.0–7.0 and the calculated monolayer adsorption capacity for the adsorption of NH_4^+ onto CTS-*g*-PAA/30 wt% HT is as high as 40.9 mg N/g, enabling it as a potentially feasible absorbent for NH_4^+ removal. This hydrogel adsorbent can be easily regenerated and the adsorption capacity cannot be affected during the regeneration process.

Acknowledgements

The authors thank the National Natural Science Foundation of China (No. 20877077) and Taihu Project of Jiangsu Provincial Science and Technology Office (No. BS2007118). for joint support.

References

1. Crini, G. (2005) *Prog. Polym. Sci.*, 30, 38–70.
2. Sun, S. and Wang, A. (2006) *Sep. Purif. Technol.*, 49, 197–204.
3. Chauhan, D. and Sankararamakrishnan, N. (2008) *Bioresource Technol.*, 99, 9021–9024.
4. Vidyalakshmi, K., Rashmi, K.N., Kumar, T.M.P. and Siddaramaiah. (2004) *J. Macromol. Sci. A*, 41, 1115–1122.
5. Dutta, P.K., Tripathi, S., Mehrotra, G.K. and Dutta, J. (2009) *Food Chem.*, 114, 1173–1182.
6. Darder, M., Colilla, M. and Ruiz-Hitzky, E. (2005) *Appl. Clay Sci.*, 28, 199–208.
7. Lin, J., He, C., Zhao, Y. and Zhang, S. (2009) *Actuat B-Chem.*, 137, 768–773.
8. Wan, Y., Peppley, B., Creber, K.A.M., Bui, V.T. and Halliop, E. (2008) *J. Power Sources*, 185, 183–187.
9. Huang, K.-S., Wu, W.-J., Chen, J.-B. and Lian, H.-S. (2008) *Carbohyd. Polym.*, 73, 254–260.
10. Liu, J., Wang, Q. and Wang, A. (2007) *Carbohyd. Polym.*, 70, 166–173.
11. Kim, I.-Y., Seo, S.-J., Moon, H.-S., Yoo, M.-K., Park, I.-Y., Kim, B.-C. and Cho, C.-S. (2008) *Biotechnol. Adv.*, 26, 1–21.
12. Crini, G. and Badot, P.M. (2008) *Prog. Polym. Sci.* 33, 399–447.
13. Zalloum, H.M., Al-Qodah, Z. and Mubarak, M.S. (2009) *J. Macromol. Sci. A*, 46, 46–57.
14. Wang, J.P., Chen, Y.Z., Zhang, S.J. and Yu, H.Q. (2008) *Bioresource Technol.*, 99, 3397–3402.
15. Prashanth, K.V.H. and Tharanathan, R.N. (2003) *Carbohyd. Polym.*, 54, 343–351.
16. Adali, T. and Yilmaz, E. (2009) *Carbohyd. Polym.*, 77, 136–141.
17. Li, A., Wang, A. and Chen, J. (2004) *J. Appl. Polym. Sci.*, 92, 1596–1603.
18. Zheng, Y. and Wang, A. (2007) *E-Polymers*, no. 127.
19. Zheng, Y., Li, P., Zhang, J. and Wang, A. (2007) *Eur. Polym. J.*, 43, 1691–1698.
20. Santiago, F., Mucientes, A.E., Osorio, M. and Poblete, F.J. (2006) *Polym. Int.*, 55, 843–848.
21. Shchukin, D.G., Sukhorukov, G.B., Price, R.R. and Lvov, Y.M. (2005) *Small*, 1, 510–513.
22. Levis, S.R. and Deasy, P.B. (2003) *Int. J. Pharm.*, 253, 145–157.
23. Viseras, M.T., Aguzzi, C., Cerezo, P., Viseras, C. and Valenzuela, C. (2008) *Micropor. Mesopor. Mat.*, 108, 112–116.
24. Lvov, Y.M., Shchukin, D.G., Möhwald, H. and Price, R.R. (2008) *ACS Nano*, 2, 814–820.
25. Ning, N.Y., Yin, Q.J., Luo, F., Zhang, Q., Du, R. and Fu, Q. (2007) *Polymer*, 48, 7374–7384.
26. Lee, S.Y. and Kim, S.J. (2002) *Appl. Clay Sci.*, 22, 55–63.
27. Wang, L., Zhang, J. and Wang, A. (2008) *Colloids Surface. A*, 322, 47–53.
28. Guo, L. (2007) *Science*, 317, 1166–1166.
29. Barrientos-Ramírez, S., Ramos-Fernández, E.V., Silvestre-Albero, J., Sepúlveda-Escribano, A., Pastor-Blas, M.M. and González-Montiel, A. (2009) *Micropor. Mesopor. Mat.*, 120, 132–140.
30. Horváth, E., Kristóf, J., Frost, R.L., Rédey, Á., Vágvölgyi, V. and Cseh, T. (2003) *J. Therm. Anal. Calorim.*, 71, 707–714.
31. Joussein, E., Petit, S. and Delvaux, B. (2007) *Appl. Clay Sci.*, 35, 17–24.